

Numerical Modeling of Flow Pattern at a Right-angled River Bend Using CCHE2D Model

Animesh Das^{1,*} Sushant Kumar Biswal² 

¹ Civil Engineering Department, National Institute of Technology, Agartala, Tripura, India

² Civil Engineering Department, National Institute of Technology, Agartala, Tripura, India

* Corresponding author: sushantb69@gmail.com

Received: 14.10.2022

Accepted: 31.01.2023

Abstract

In this study, the CCHE2D model is used to analyse the flow pattern in a meander reach of the Gomati River. The finite volume method is used by the numerical model to solve the depth-averaged two-dimensional equations with $k - \epsilon$ turbulence closure. The numerical findings were compared with field data for two different flow rates in order to calibrate the CCHE2D model using various Manning's roughness coefficients. The results show that for the minimum and maximum discharges, a smaller Manning's roughness factor ($0.015 \geq n \geq 0.025$) is more favorable to a higher Manning's roughness factor ($0.030 \leq n \leq 0.040$). The results of the numerical model demonstrated that fluctuations in hydraulic parameters including shear stress, velocity, flow depth, and Froude number in the river bend are greatly influenced by the existence of centrifugal force and helical cells. The linear relationship between velocity and shear stress is presented across the whole study reach, as indicated by the R-square and linear correlation coefficient (r) components. The results of the model show that the flow field within the river bend can be accurately simulated by the computational model.

Keywords: Gomati River; CCHE2D; Manning's coefficient; meander reach

1. Introduction

One of the most common river patterns found in nature are meandering rivers, which are formed into different shapes by rivers due to their dynamic character. Its platform is always changing, and these changes have a big impact on the morphology and hydraulic condition. Meandering rivers are single channels with a sinuous planform composed of a succession of loops that are often irregular, asymmetrical, and complex in reality though being shown as having regular form and size (Hooke, 2013). The effects of secondary flow, free surface variation, section geometry, and flow separation along the inner bend wall, which are not seen along straight paths, combine to produce extremely complex three-dimensional (3D) flows in meander rivers or river bends. One of the key aspects of open channel flows is the distribution of flow velocity in the longitudinal and lateral directions. This aspect is related to a variety of flow characteristics, such as the water profile, the distribution of shear stress, secondary flow, channel conveyance, and other flow entities. Secondary currents are one of the important characteristics that define flow in meander bends. According to Chang (1984),

even for small curves without flow separation, flow resistance or the energy cost caused by transverse flow can be extremely large. Many researchers have studied flow dynamics in a wide variety of channel bend configurations using various methods owing to the major significance of this content (Tominaga and Nagao, 2000; Blanckaert and Graf, 2001; Booij, 2003; Blanckaert and De Vriend, 2004; Lu et al., 2004; Bodnar and Prihoda, 2006; Roca et al., 2007; Blanckaert, 2009; Zhou et al. 2009). These studies aim to collect data on flow variables in channel bends and analysis of the results that have provided the knowledge base for understanding the bend flows. Due to improvements in computers and numerical computation techniques, Computational Fluid Dynamics (CFD) models have seen a substantial increase in use in recent decades for studying outdoor channels and river dynamics. In order to solve difficult hydrodynamic issues, numerical models have been applied widely at different scales. Various types of numerical models have been employed to explain the details of flow within bends and meandering channels using different turbulence modelling techniques, such as the direct numerical simulation (DNS), large eddy simulations (LES), or the Reynolds-Averaged Navier-Stokes (RANS) approach. Ye and Mccorquodale (1998) simulated the flow and mass transfer in a 270° curved channel using a mathematical model of 3D free surface flows. A fractional three-step implicit algorithm uses a collocated grid system to solve the governing equations. A two-dimensional (2D) numerical model was used by Lien et al. (1999) to study the flow pattern at a 180° bend with a rigid bed. They found that the secondary flow significantly affects the flow patterns and the path of maximum velocity along the channel. Huang et al. (2009) used various pressure solution techniques along with different turbulence closure methods, to evaluate the spiral flows in an experiment's curved channel, use models like the $k - \varepsilon$ model and the mixing-length model. To understand hydrodynamics sedimentation and its transport mechanism, a general tool CCHE2D was developed by National Center for Computational Hydro Sciences and Engineering (NCCHE), University of Mississippi. CCHE2D is widely used by the riverine scientist for sediment and flow modelling Singh (2005); Kamanbedast (2013). CCHE2D model has been used for simulation at the Nile River (Elbogdady reach), and multi parametric sensitivity with different roughness parameters were evaluated using RSQ and r factors (Nassar, 2011). Mohanty et al. (2012) investigated wide meandering compound channels using CCHE2D to analyse the depth-averaged velocity. The results indicated that centrifugal force and secondary flow have a significant impact on the flow patterns in a channel bend. The maximum velocity in the main channel is closer to the inner bend whether it is above or below the bank level, according to McKeogh and Kiely's (1989) analysis of the velocity profile in meandering compound rivers. Elyasi and Kamandbedast (2014) used the CCHE2D model to investigate numerical modeling of river flow with a 90 degree bend. The results of flow pattern simulations in meandering sections using the CCHE2D model in the Khoshke-rud river in Iran show that using numerical flow simulations for flow modeling is a step closer to being a universal predictor of processes in meandering rivers (Fathi et al., 2012). Yusefi Haghivar et al. (2017) used CCHE2D model to investigate the hydraulic parameters of flow depth and velocity in the Karoon River, Iran. Ultimately, it became clear that there was a subtle harmony between changes in river depth and flow, with most changes occurring in meanders and bends. Scott and Jia (2005) concluded that CCHE2D is capable of simulating both hydrodynamic and sediment properties of complex river network and has proved the model as a valuable tool for engineering projects. Current study performs flow analysis in the meander reach of the Gomati River using the CCHE2D modelling software.

A review of the literature shows that there are few comprehensive studies of 2D numerical modelling of meandering flow. The goal of this work is to analyse earlier studies that assessed a river meander's flow characteristics using numerical techniques. In the present

study, the flow pattern of the Gomati River is analysed using the most recent CCHE2D modelling software. This study utilizes a numerical model that solves the 2D depth-averaged conservation equations to examine the flow characteristics of a meander reach with a 90° angled bend for the Gomati channel. The main goals of this study are to analyse the flow patterns in meander reaches and to measure various hydraulic parameters in the Gomati River study course, including shear stress, total specific discharge, velocity, and Froude number. Different Manning's roughness coefficients are used as the initial conditions to calibrate the CCHE2D model for the Gomati River flow simulation, and simulation results are compared with measured flow data.

2. Materials and Methods

2.1 Study Area

The Gomati River, 56 kilometers south-west of Agartala, is the site of a significant field project on the river bend that includes in this study (Figure 1). The Gomati catchment covers 2492 km² (1921 km² belongs to hilly region and only 571 km² about 23% lies on the plain) is located in the lower middle part of Tripura. It is located between 23°47'N and 23°47'N in latitude and 91°14'E and 91°58'E in longitude. The Gomati River is the largest river of State of Tripura, India and the river is 167.4 kilometers in length, with an elevation range of 18.288 to 112.166 meters above mean sea level.

Table 1. Physical parameters of the present study.

Stream length (s_L), m	Valley length (V_L), m	Width (B), m	Bed slope (S)	Angle (β), degree	Radius of curvature (R_C), m	Sinuosity (K)
94.62	53.16	42.7	0.0006	90	60.22	1.78

The Gomati River's 94.62 m bend is used in the current study for flow simulation to understand the behavior of river flow dynamics. A bathymetric survey was carried out to obtain information at the study site under consideration. Hydrologic data were collected throughout the field campaign at upstream stage recorders, and were converted to discharge values using stage-discharge rating curves (Figure not shown). The rating curve is the relationship between stage (river water level) and streamflow (discharge). A rating curve was established, because at many channel locations, the discharge is not a unique function of stage; but also the slope of the water surface, the channel geometry, and the unsteadiness of flow. So, the rating relationship thus established is used to transform the observed stages into the corresponding discharges. Field data is analyzed analytically and compared to stage record data.

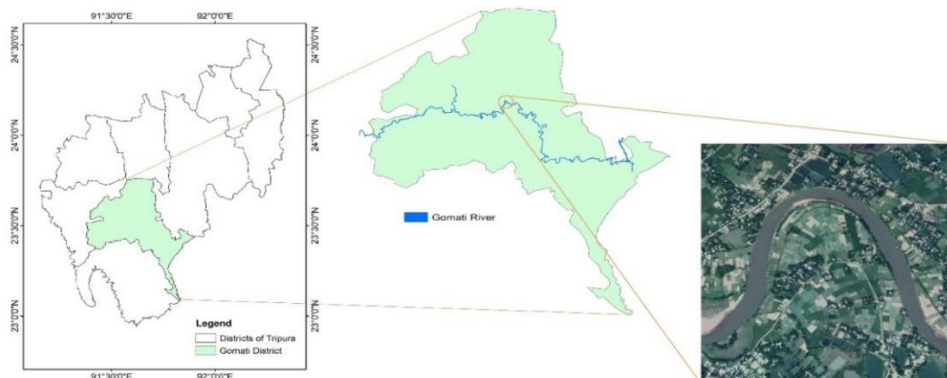


Figure 1. Location map of the considered reach of Gomati River

2.2. CCHE2D Model

The CCHE2D model is a comprehensive software programme for the 2D modelling and analysis of morphological phenomena and free surface flows. Figure 2 shows the flow chart for the flow simulation modelling process utilising the digital elevation model and the integration of CCHE2D models and Arc GIS. The package comprises of the numerical models, a mesh generator (CCHE2D Mesh Generator) and a Graphical User Interface (CCHE2D-GUI). For the CCHE2D model system, the mesh generator helps in the formation of a complex structured mesh system. The CCHE2D series, which includes the grid generator and CCHE2D-GUI, was used to create a topographical file that could be loaded as part of the modelling procedure. In the earlier, each of the flow data is input using a flow input device, which is then utilised to do analysis and show the results. In the former, topographic data are used to construct a mesh. The digital elevation topography data received that was clipped in ArcGIS primarily contained the river bend that is significant for the overbanks. The Digital Elevation Model (DEM) was cropped and then converted to ASCII output in order to be input into CCHE2D Model Generator. After the topography data was loaded into the CCHE2D grid generator, the block defining the boundaries of the river was generated. The mesh generating toolbar was used to discretize the algebraic mesh created from the topography into finer meshes. A minimum number of dry grid cells were used with arbitrary initial flow parameters, such as the initial depth of the water surface at the river inflow and outlet. The water surface level was interpolated using the interpolation tool in the set flow beginning conditions toolbar. The roughness characteristics were entered into the CCHE2D-GUI with probable values for the overall topography. The water surface level and flow discharge were set using intake boundary condition and outlet boundary condition, respectively, in the current study. Ten-second time steps were utilised to simulate an entire day. This study only utilise the hydraulics capability of CCHE2D.

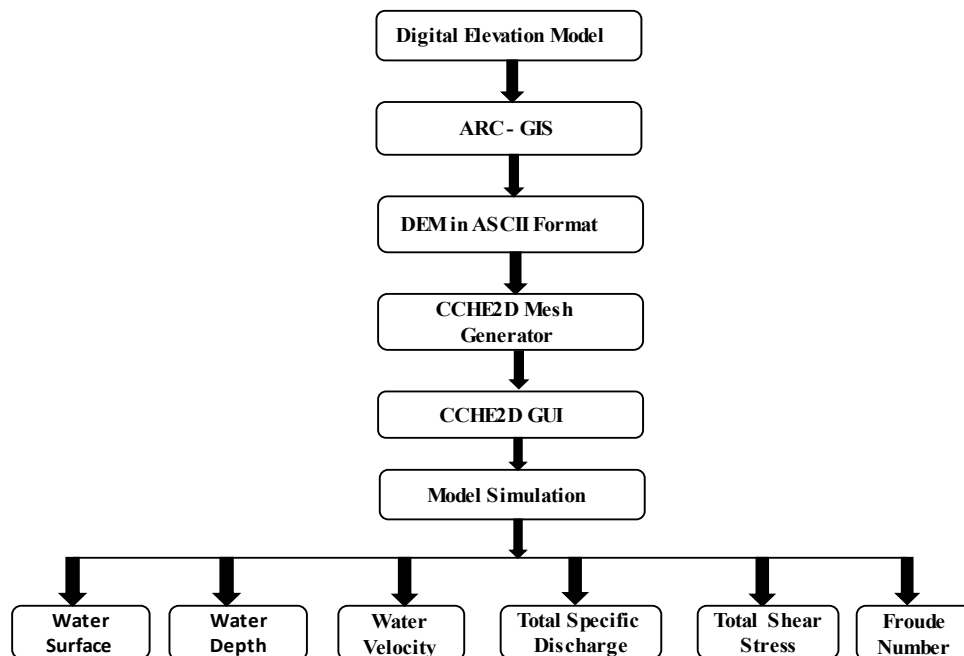


Figure 2. Flow chart shows the operations involved in the flow simulation modelling with the digital elevation model and the combination of Arc GIS and CCHE2D models

2.3 Numerical Method

Numerical model was applied to solve depth-averaged two-dimensional conservation equations with $k - \varepsilon$ turbulence closure using CFD software (CCHE2D) model. In the

present study, the Finite volume method (FVM) with the second order upwind scheme is used to discretize the governing equations. The governing 2D continuity and momentum equations for an incompressible fluid flow are written as Eq. (1), Eq. (2) and Eq. (3):

$$\begin{array}{l} \text{Continuity} \\ \text{Equation} \end{array} \quad \frac{\partial z}{\partial t} + \frac{\partial(hu)}{\partial x} + \frac{\partial(hv)}{\partial y} = 0 \quad (1)$$

$$\begin{array}{l} \text{Momentum} \\ \text{Equations} \end{array} \quad \frac{\partial u}{\partial t} + u \frac{\partial u}{\partial x} + v \frac{\partial u}{\partial y} = -gh \frac{\partial z}{\partial x} + \frac{1}{h} \left[\frac{\partial(h\tau_{xx})}{\partial x} + \frac{\partial(h\tau_{xy})}{\partial y} \right] - \frac{\tau_{bx}}{\rho h} + f_{Cor} v \quad (2)$$

$$\frac{\partial v}{\partial t} + u \frac{\partial v}{\partial x} + v \frac{\partial v}{\partial y} = -gh \frac{\partial z}{\partial y} + \frac{1}{h} \left[\frac{\partial(h\tau_{yx})}{\partial x} + \frac{\partial(h\tau_{yy})}{\partial y} \right] - \frac{\tau_{by}}{\rho h} + f_{Cor} u \quad (3)$$

where u and v are depth integrated velocity components in x and y directions respectively, g is gravitational acceleration, z is the water surface elevation, ρ is water density, h is the local water depth, f_{Cor} is the Coriolis parameter, τ_{xx} , τ_{xy} , τ_{yx} and τ_{yy} are the depth integrated Reynolds stresses and τ_{bx} , τ_{by} are shear stresses on the bed surface. The Coriolis parameter f_{Cor} was ignored in this analysis because it has no significant influence for small areas (Dutta et al., 2010).

The DEM, river location, initial water surface elevation, discharge, and Manning's roughness coefficient are the basic input data requirements for operating the CCHE2D model. In addition to the initial conditions, the boundary conditions are applied at the inlet and outlet sections. The flow discharge was defined as a constant value for simulation as the inlet boundary condition, and the water surface level was defined for the model as a outlet boundary conditions. Grids to represent flow depth and flow velocity at any time increment specified by the user compensate the CCHE2D model's output. Grid sensitivity study has been performed to work out the specified number of grid points and their distribution by refining the grid points.

4. Results and Discussions

DEM file in ASCII format was gridded numerically and algebraically. The export results from the mesh editor are given in Figure 3 that shows the bed elevation with minimum and maximum values of 32.79 m and 67.24 m, respectively. The CCHE2D mesh generator was used to interpolate the bed height at random. In order to reduce adverse depths, the beginning water level was higher than 32.79 m for the purpose of this study. The results of the CCHE2D-GUI's flow simulation are shown in Figure 4. The largest long-term monthly average is shown together with the water surface elevation in metres after a simulation time longer than a day.

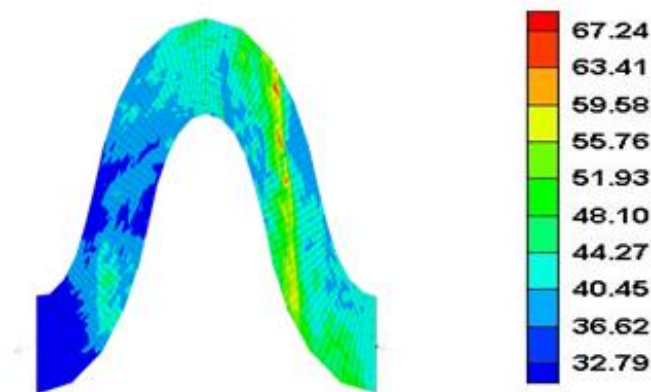


Figure 3. Initial bed elevation (m) generated by CCHE2D

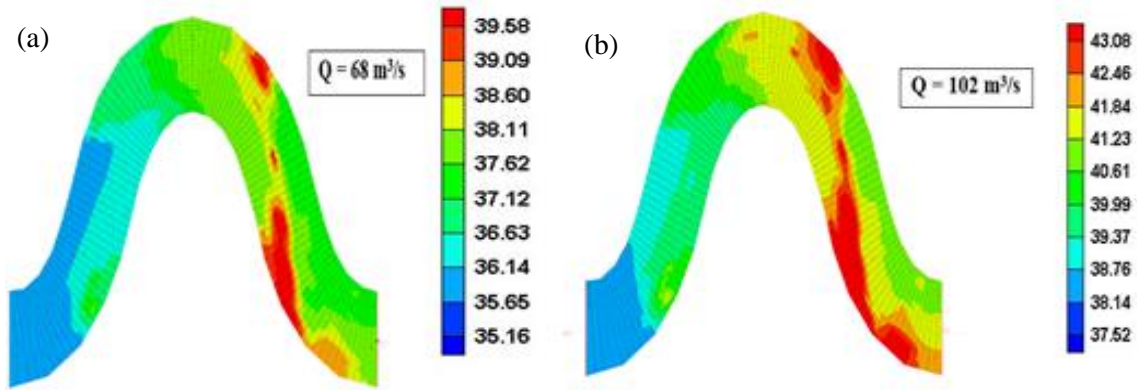


Figure 4. Water surface profile at 90° meander (a) Q=68 m³/s, (b) Q=102 m³/s

In various cross sections of the 90° river bend from the study stretch, Figure 5 shows the cross-profiles of the water surface computed from the CCHE2D numerical model. Due to the presence of secondary currents in the bend, the gradient of the water surface increases to the outer bank. The results show that at a flow of 102 m³/s, the water surface level rises upstream and attain maximum depth of 6.38 m, while the water depth at the edge of the river is almost zero. The large depth provides information about the size of the river carrying a significant amount of flow. Using more reliable inputs, such as bathymetric data, which can modify the depth results and provides more accurate data on the submerged surfaces. The maximum water depth, specific discharge, velocity, Froude numbers and total shear stress are reached very near the centreline of river. The results show that the minimum water depth for the reach of study is 0.001 m, and the associated low-depth zones, there is no stream velocity. The muddy area inside the Gomati boundaries, where the discharge is most likely to occur on a long-term monthly average, is shown by this depth. The numerical results demonstrate that as flow enters the curve, centrifugal force leads the water surface to locate a transversal slope. Figure 6 shows the water depth profiles based on six roughness coefficients of 0.015, 0.020, 0.025, 0.030, 0.035, and 0.040 that were obtained from the CCHE2D model and observed data. It can be shown that both the water depth profiles of numerical model and the observational data show a regular trend for different roughness coefficients. The water depth profile of the Gomati River reach was analysed in order to find the optimum roughness coefficient. Two components of the linear correlation coefficient r and coefficient of determination (R^2), as specified by Eq. (4) and Eq. (5), were used in statistical analysis to compare the observed and simulated data for all tests in accordance with Figure 6.

$$\text{Correlation } (r) = \frac{N \sum AB - (\sum A \sum B)}{[(N \sum A^2) - (\sum A)^2] [N \sum B^2 - (\sum B)^2]^{0.5}} \quad (4)$$

$$\text{RSQ } (R^2) = \frac{\sum_i^j (B - \bar{A})^2}{\sum_i^j (A - \bar{A})^2} \quad (5)$$

where B is the simulated variable, A is the observed variable, \bar{A} is the sample mean of A value, and N the total number of variables.

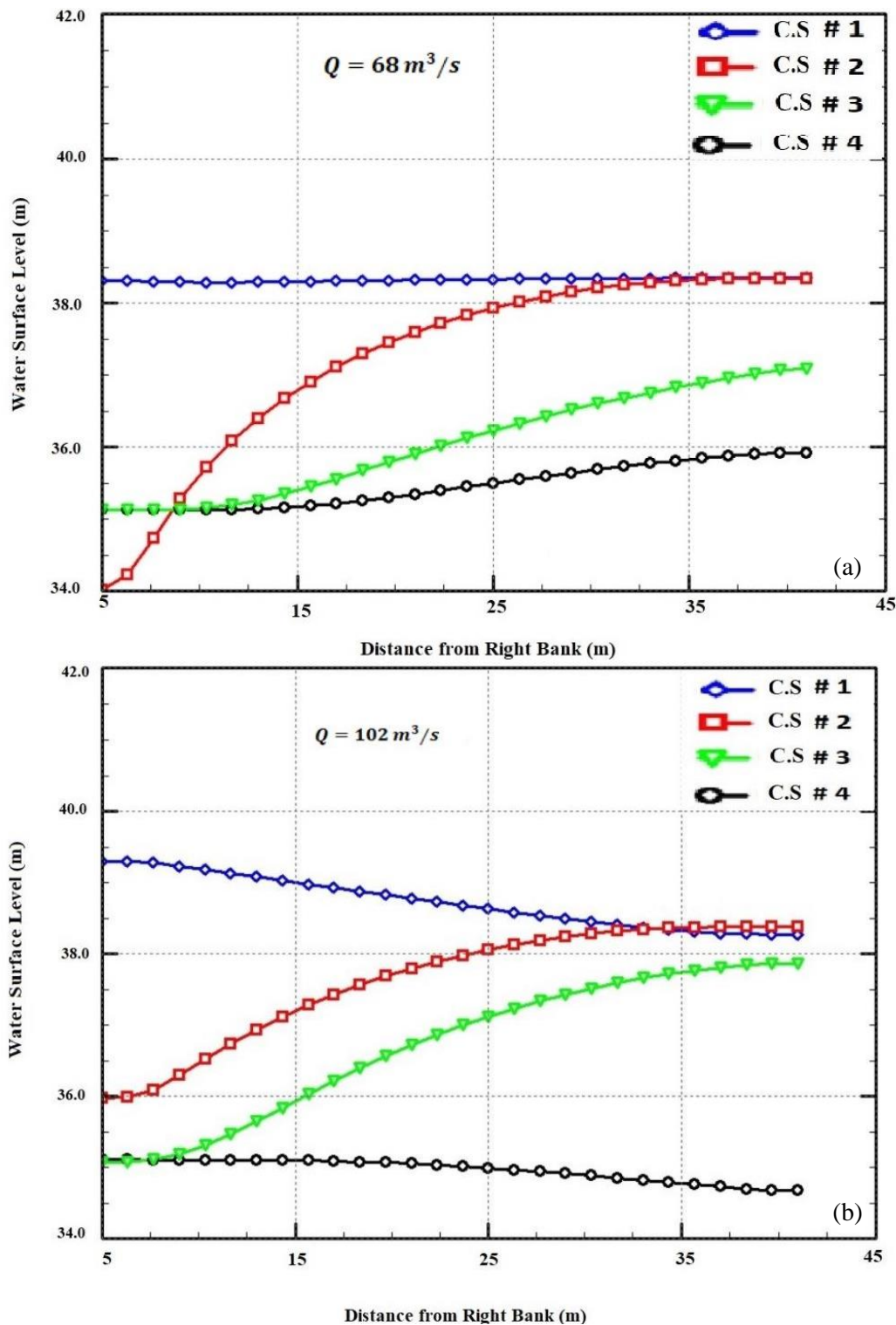


Figure 5. Cross-profiles of water surface at 90° meander (a) $Q=68 \text{ m}^3/\text{s}$, (b) $Q=102 \text{ m}^3/\text{s}$

Figure 7 shows that Manning’s roughness coefficients for low and high discharges ($68 \text{ m}^3/\text{s}$ and $102 \text{ m}^3/\text{s}$) lie within in the range of $(0.015 \geq n \geq 0.025)$. Due to the higher roughness coefficients ($0.030 \geq n \geq 0.040$) and smaller depth for modelling, it can be said that the impact of roughness of the bed on flow is greater for low discharge and that the results are better and more accurate when compared to observational data. Therefore, lower roughness coefficients are more acceptable for low and high discharges.

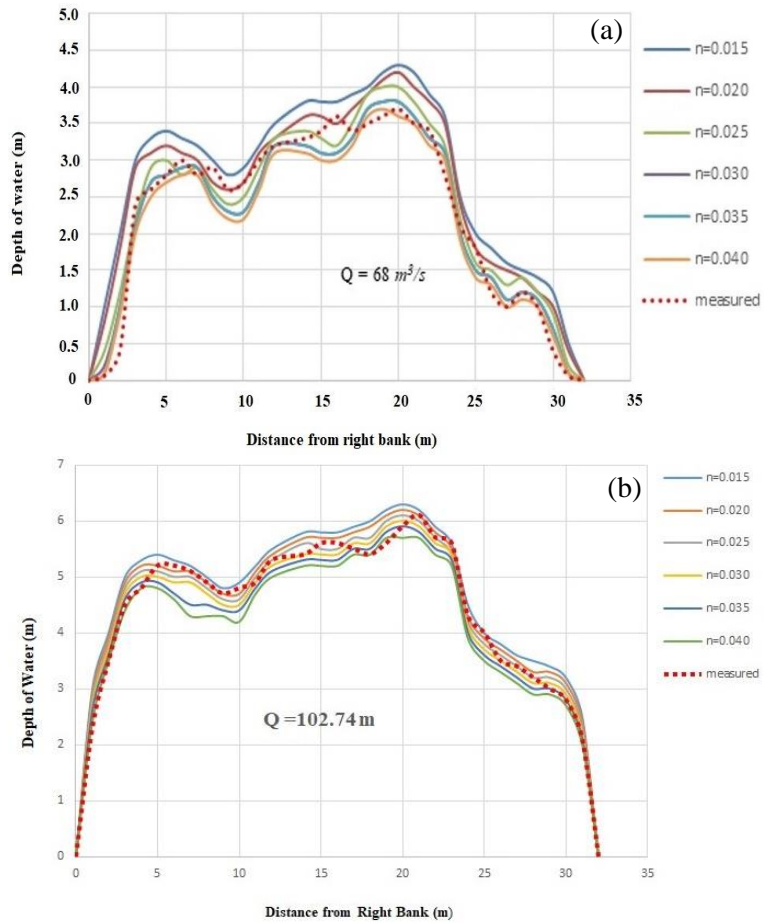


Figure 6. Water depth elevation at 90° meander (a) $Q=68 \text{ m}^3/\text{s}$, (b) $Q=102 \text{ m}^3/\text{s}$

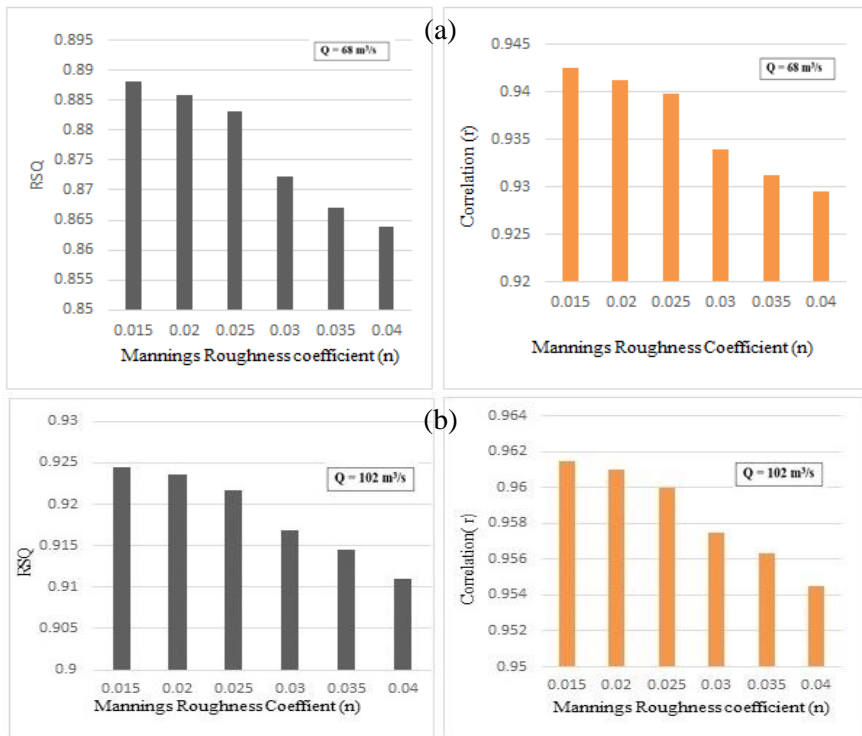


Figure 7. The performance of the CCHE2D model for different Manning's roughness coefficients (a) $Q=68 \text{ m}^3/\text{s}$, (b) $Q=102 \text{ m}^3/\text{s}$

Figure 8 shows the velocity profile for a specific discharge along the meandering path through the channel. In the early stages of the meander path, the region of still higher velocity is along the inner wall to the left of the channel section. The higher velocity moves toward the middle of the channel during the cross-over section, as is usually observed in straight channels. Based on this observation, a meandering channel acts like a straight channel just before the cross-over section. The higher velocity goes to the right of the channel section at sections after the cross-over; this is outer wall of the channel section (Figure 9).

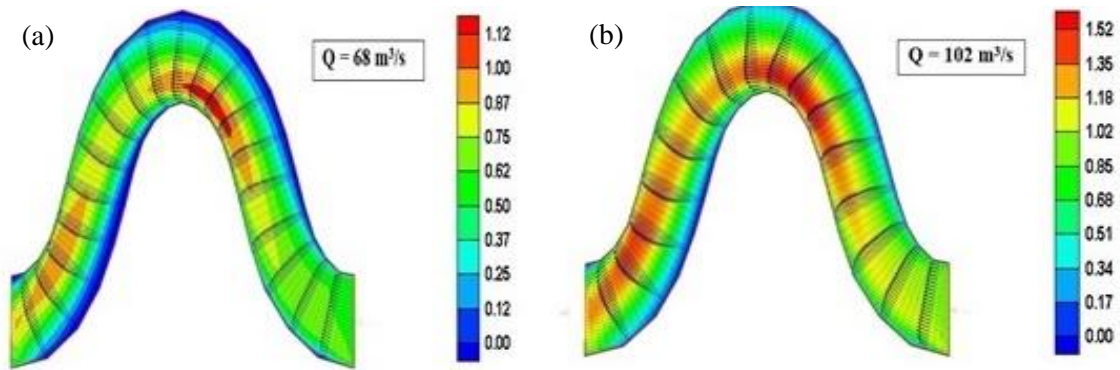


Figure 8. Velocity vector at 90° meander (a) $Q=68 \text{ m}^3/\text{s}$, (b) $Q=102 \text{ m}^3/\text{s}$

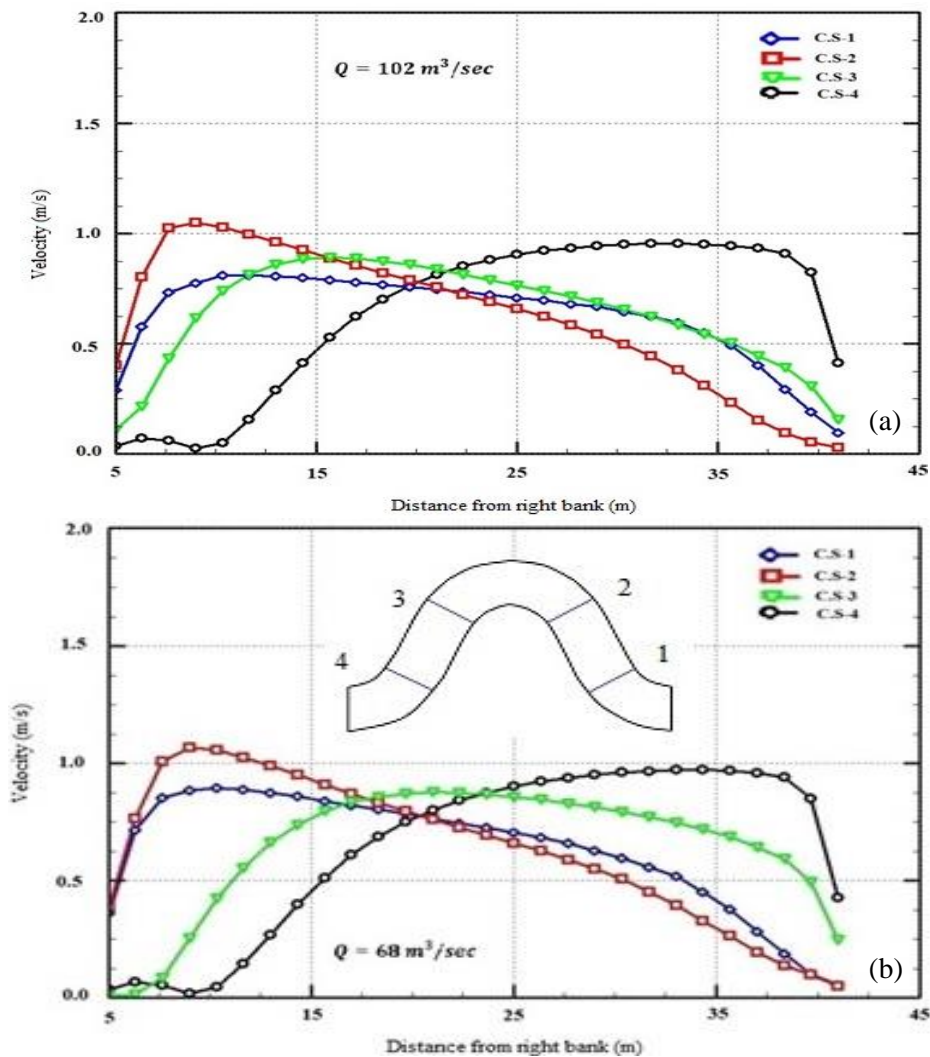


Figure 9. Cross-profiles of velocity at 90° meander for 102 m^3/s discharges (a) $Q=68 \text{ m}^3/\text{s}$, (b) $Q=102 \text{ m}^3/\text{s}$

The boundary shear force distribution along the channel bed directly affects the flow characteristics of an open channel flow. Throughout the bend, the shear stress generally increases with flow and peaks at its highest levels during the highest discharge (Figure 10).

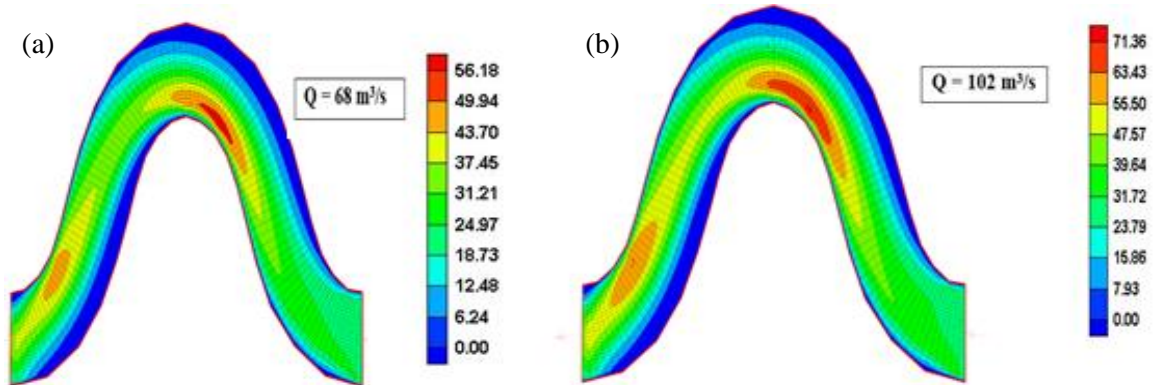


Figure 10. Shear stress at 90° meander (a) $Q=68 \text{ m}^3/\text{s}$, (b) $Q=102 \text{ m}^3/\text{s}$

The total specific discharge (m^2/s) is at its highest along the centreline of the river, as per Figure 11 of the present work, that examines the influence of parameters like specific discharge and Froude number on the flow dynamics.

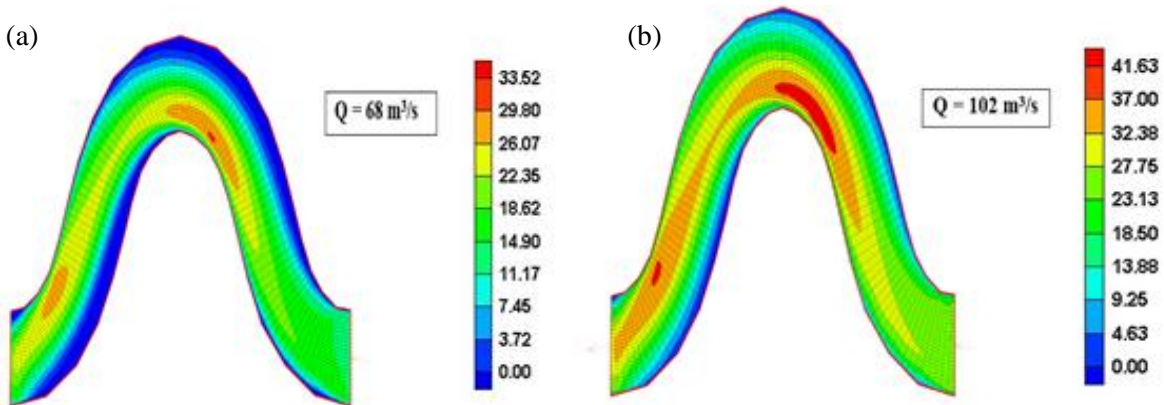


Figure 11. Total specific discharge at 90° meander (a) $Q=68 \text{ m}^3/\text{s}$, (b) $Q=102 \text{ m}^3/\text{s}$

Figure 12 shows the Froude number mapping, which indicates that the flow in the upstream reach is subcritical ($Fr < 1$), but that it becomes supercritical ($Fr > 1$) as a result of the obstruction in the contraction area upstream. The current study confirmed that the majority of the flow in the channel reach is subcritical.

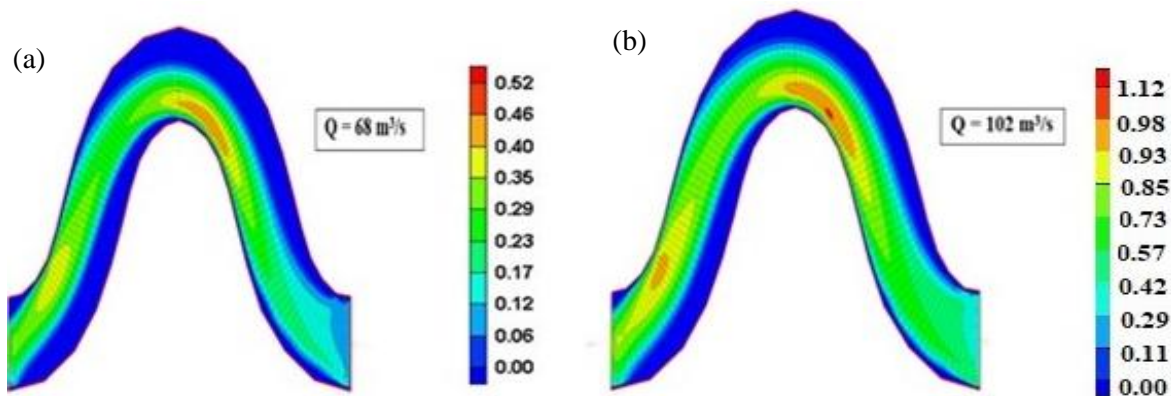


Figure 12. Froude number at 90° meander (a) $Q=68 \text{ m}^3/\text{s}$, (b) $Q=102 \text{ m}^3/\text{s}$

4. Conclusions

In this study, the flow attributes at a Gomati River bend have been numerically solved using the CCHE2D model. The numerical results were simulated using field data. According to the model results, the roughness factor values of 0.030–0.040 will have better results, and for medium and high discharges, the roughness factor ranges of 0.015–0.025 will provide results that are more accurate. The simulation results also imply that, the average velocity for the discharges of 68 m³/s and 102 m³/s in the study reach is 0.56 m/s and 0.77 m/s, respectively. Additionally, the average shear stress for the two discharges mentioned above is 27.99 and 35.62 N/m², respectively. The analysis demonstrates that the water surface and the highest velocities in the river arch evolve toward the outer bank. The present study results show that the model is efficient to simulate wide range of flow parameters in riverine system and can better predict sedimentation and erosion. Therefore, the results of this numerical models are reliable and useful in the engineering and operational projects of the Gomati River.

Acknowledgments

The authors would like to thank National Institute of Technology Agartala for providing financial support in completing this study and would like to thank International Conference on Hydrosience and Engineering (ICHE) for the opportunity to publish this work.

Conflict of Interest

The authors declare no conflict of interest.

References

- Blanckaert, K. (2009). Saturation of Curvature-Induced Secondary Flow, Energy Losses, and Turbulence in Sharp Open-Channel Bends: Laboratory Experiments, Analysis, and Modeling. *J. Geophys. Res. Earth Surf.*, 114.
- Blanckaert, K., & Graf, W. H. (2001). Mean Flow and Turbulence in Open-Channel Bend. *J. Hydraul. Eng.*, 127, 835–847.
- Blanckaert, K., & De Vriend, H. J. (2004). Secondary Flow in Sharp Open-Channel Bends. *J. Fluid Mech.*, 498, 353–380.
- Bodnar, T., & Prihoda, J. (2006). Numerical Simulation of Turbulent Free-Surface Flow in Curved Channel. *Flow Turbul. Combust.*, 76, 429–442.
- Booij, R. (2003). Measurements and Large Eddy Simulations of the Flows in Some Curved Flumes. *J. Turbul.*, 4, 1–17.
- Chang, H. H. (1984). Variation of Flow Resistance through Curved Channels. *J. Hydraul. Eng.*, 110(12), 1772–1782.
- Dutta, S., Medhi, H., Karmaker, T., Singh, Y., Prabu, I., & Dutta, U. (2010). Probabilistic Flood Hazard Mapping for Embankment Breaching. *ISH Journal of Hydraulic Engineering*, 16(1), 15–25 <https://doi.org/10.1080/09715010.2010.10515012>.
- Fathi, M., Honarbakhsh, A., Rostami, M., Nasri, M., & Moradi, Y. (2012). Sensitive Analysis of Calculated Mesh for CCHE2D Numerical Model. *World Appl Sci J.*, 18, 1037–1051.
- Hooke, J. M. (2013). Chapter: River meandering. In *Treatise on Geomorphology* San Diego, CA: Academic Press, 260–288.

- Huang, S., Jia, Y., Chan, H., & Wang, S. S. Y. (2009). Three-Dimensional Numerical Modeling of Secondary Flows in a Wide Curved Channel. *J. Hydrodynamics.*, 21(6), 758-766.
- Kamanbedast, A. A., Nasrollahpour, R., & Mashal, M. (2013). Estimation of Sediment Transport in Rivers Using CCHE2D Model (Case Study: Karkheh River). *Indian Journal of Science and Technology*, 6(2), 138-14 DOI:10.17485/ijst/2013/v6i2.9.
- Lien, H. C., Yang, J. C., Yeh, K. C., & Hsieh, T. Y. (1999). Bend-Flow Simulation Using 2D Depth-Averaged Model. *Journal of Hydraulic Engineering*, 125(10), 1097-1108.
- Lu, W., Zhang, W., Cui, C., & Leung, A. (2004). A Numerical Analysis of Free-Surface Flow in Curved Open Channel with Velocity-Pressure Free-Surface Correction. *Comput. Mech.*, 33, 215-224.
- McKeogh, E. J., & Kiely, G. K. (1989). Experimental Study of the Mechanisms of Flood Flow in Meandering Channels, *Proceedings of the 23rd IAHR Congress*, 491-498.
- Mohanty, P. K., Dash, S. S., & Khatua, K. K. (2012). Flow Investigations in a Wide Meandering Compound Channel. *Int. J. Hydraul Eng.*, 1(6), 83- 94.
- Nassar, M. A. (2011). Multi-parametric Sensitivity Analysis of CCHE2D for Channel Flow Simulation in Nile River. *J. Hydro. Environ. Res.*, 5, 187-195
- Roca, M., Martin Vide, J. P., & Blanckaert, K. (2007). Reduction of Bend Scour by an Outer Bank Footing: Footing Design and Bed Topography. *J. Hydraul. Eng.*, 133, 139-147.
- Scott, S. H., & Jia, Y. (2005). Simulation of Sediment Transport and Channel Morphology Change in Large River Systems. *Us-China Workshop On Advanced Computational Modelling In Hydrosience & Engineering*.
- Singh, V. (2005). Two Dimensional Sediment Transport Model Using Parallel Computers. *Doctoral Dissertation*, Faculty of the Louisiana State University and Agricultural and Mechanical College in partial fulfillment of the requirements for the degree of Master of Science in Civil Engineering in The Department of Civil and Environmental Engineering by Vikas Singh B. Tech., Banaras Hindu University, India.
- Tominaga, A., & Nagao, M. (2000). Secondary Flow Structure in Bends of Narrow Open Channels with Various Cross Sections. *Proceedings of the 4th International Conference on Hydrosience and Engineering*, Seoul, Korea, 26-29 September 2000.
- Ye, J., & Mccorquodale, J. A. (1998). Simulation of Curved Open Channel Flows by 3D Hydrodynamic Model. *J. Hydraul. Eng.*, 124(7), 687-698.
- Yusefi Haghivar, M., Behdarvandi Askar, M., Moalemi, S. (2017). Investigation Flow Depth and Flow Speed Changes in the Karun River. *Open J. Mar. Sci.*, 7, 289-299. <https://doi.org/10.4236/ojms.2017.72021>